PAPER

Deflectometric systems for absolute flatness measurements at PTB

Meas. Sci. Technol. **23** (2012) 094007 (8pp) doi:10.1088/0957-0233/23/9/094007

Deflectometric systems for absolute flatness measurements at PTB

G Ehret[1], **M Schulz**[1], **M Stavridis**[2] **and C Elster**[2]

[1] Physikalisch-Technische Bundesanstalt, Bundesallee 100, 38116 Braunschweig, Germany
[2] Physikalisch-Technische Bundesanstalt, Abbestr. 2-12, 10587 Berlin, Germany

E-mail: gerd.ehret@ptb.de

Received 30 November 2011, in final form 31 January 2012
Published 25 July 2012
Online at stacks.iop.org/MST/23/094007

Abstract
Recently, two new scanning deflectometric flatness reference (DFR) measurement systems were installed at the Physikalisch-Technische Bundesanstalt. These instruments are aimed at measurements of the absolute flatness of optical surfaces with sub-nanometre uncertainties. System 1 is mainly designed for horizontal specimens with sizes up to 1 m and weights up to 120 kg. The other setup, i.e. system 2, is designed for vertical specimens. The two DFR systems use three different deflectometric procedures, which are based on scanning a pentaprism or the so-called double mirror unit (DMU) across the specimen. These 90° beam deflectors eliminate—to a great extent—residual guidance errors of the scanning stages, which is required to attain topography measurements with sub-nanometre uncertainty. The setups of the two new systems, the principles of the three different measurement modes, the alignment procedures, simulation results and first measurements are presented.

Keywords: flatness measurement, deflectometry, angle measurement

(Some figures may appear in colour only in the online journal)

1. Introduction

Highly accurate flatness measurements are needed for many optical components, such as optical flats, mirrors, synchrotron optics or precision astro-optics. For example, the measurement of grazing incidence optics used in synchrotrons requires highest accuracies. For this purpose, angle-based measurement systems like long trace profilers (LTP) [1], the Nanometre Optical Metrology (NOM) system at BESSY [1] or the Diamond-NOM [2] are applied. Figure 1 shows typical flatness standards made up of Zerodur.

The absolute measurement of flat surfaces is commonly based on deflectometric or interferometric procedures. Interferometric procedures typically use the so-called three-flat test [3–7], which consists of several Fizeau interferometric measurements of the three flats in different combinations. The standard three-flat test results in an absolute topography only for a single radial line across the specimen. If one of the flats is rotated between the measurements, the absolute topography is obtained for as many radial lines as the number of rotational steps. The three-flat test has intrinsic problems for horizontally orientated specimens, since in one of the combinations one flat must be flipped upside down, thereby bending differently due to gravitation. In principle, this effect can be estimated by finite-element methods (FEM), but the FEM calculations have accuracies only in the nanometre range [8]. Hence, the three-flat test cannot be used for highly accurate flatness measurements with uncertainties in the single figure nanometre range or even below. In deflectometry, the specimen is scanned by a collimated optical beam and the deflection angle of the reflected beam is measured from which the topography is obtained by integration. Measurement uncertainties in the sub-nanometre level can be achieved [9]. Absolute measurements are achieved by exploiting the straightness of light propagation and the basic reflection law. Traceability of the measurements is obtained by calibrating the angle measurement device using a national angle reference, e.g., the primary national standard WMT 220 of Physikalisch-Technische Bundesanstalt (PTB) [10, 11]. The traceability chain is illustrated in figure 2.

The lateral resolution of typically 3 mm is determined by the aperture of the angle measurement device, e.g., the Elcomat 3000 (Moeller Wedel Optical GmbH). In contrast, interferometric procedures have the advantage of achieving

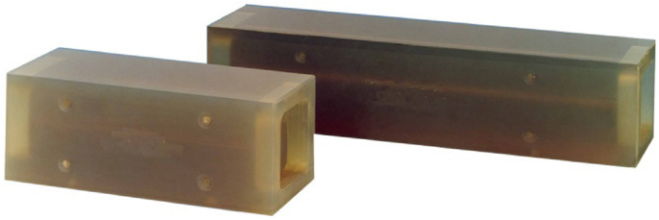

Figure 1. Flatness standards made up of Zerodur with lengths of 310 and 510 mm.

higher lateral resolution, which depends on the size of the specimen and the pixel number of the image sensor. For instance, for a specimen with a diameter of 500 mm and a 1 k image sensor, a resolution of 0.5 mm is achieved.

The main advantage of the deflectometric procedures is that much lower uncertainties in comparison to interferometric procedures can be achieved. Two new systems have therefore been set up at PTB [12, 13]. The objectives of the deflectometric systems are the provision of absolute flatness measurements of large specimens with weights up to 120 kg and dimensions up to 1000 mm. For a typical peak-to-valley height of the specimens of less than 200 nm, uncertainties in the sub-nanometre range—even for large specimens—shall be achieved. Measurements of horizontally and vertically orientated specimens are possible.

2. The setup of the two new deflectometric systems

Figure 3 shows photos of system 1, which is designed to measure horizontally oriented specimens. The housing reduces angle measurement noise caused by air turbulence. A high-precision air-bearing stage is used to move two carriages, one of which carries the autocollimator and the other the double mirror unit. The scan axis with its air bearings has positional errors of 1 micrometre and angular errors of 1 arcsec for a scan length of up to 1 m. The DMU can be aligned with respect to the optical axis in pitch, yaw and roll angles with arcsec accuracy (see section 5). The specimen can be aligned perpendicularly to the optical beam by means of two piezoactuators with a travel range of 10 μm and accuracies of some nanometres.

Figure 4 shows system 2, which is used for vertically oriented specimens. The sensor head, consisting of the autocollimator, the DMU and the shearing stage, can be scanned across the specimen. For the alignment of the DMU, a three-axis rotational positioner (Luminos Industries, RYP3000) with resolutions in the sub-arcsecond range is used.

3. Three different deflectometric measurement modes

The two systems use different deflectometric measurement modes, the so-called direct deflectometry, difference deflectometry and exact autocollimation deflectometric scanning (EADS) modes.

(1) In *direct deflectometric* mode, the surface under test is scanned with the DMU (see figure 5). The pentaprism-based arrangement of the double mirror eliminates guidance errors of the scanning stage to the first order. The autocollimator measures the slopes of the surface

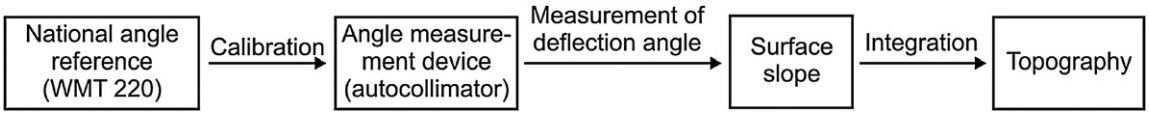

Figure 2. Traceability chain of deflectometric procedures.

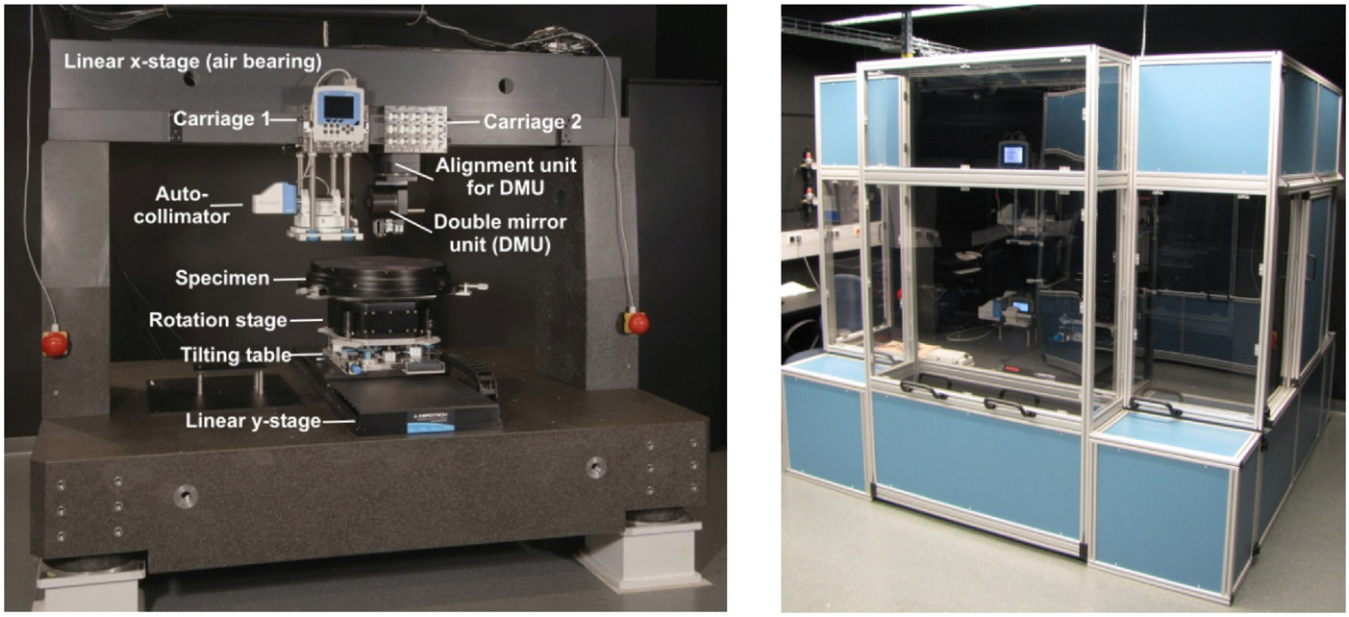

Figure 3. Photos of system 1 for horizontal specimens (*left*: without housing; *right*: with housing).

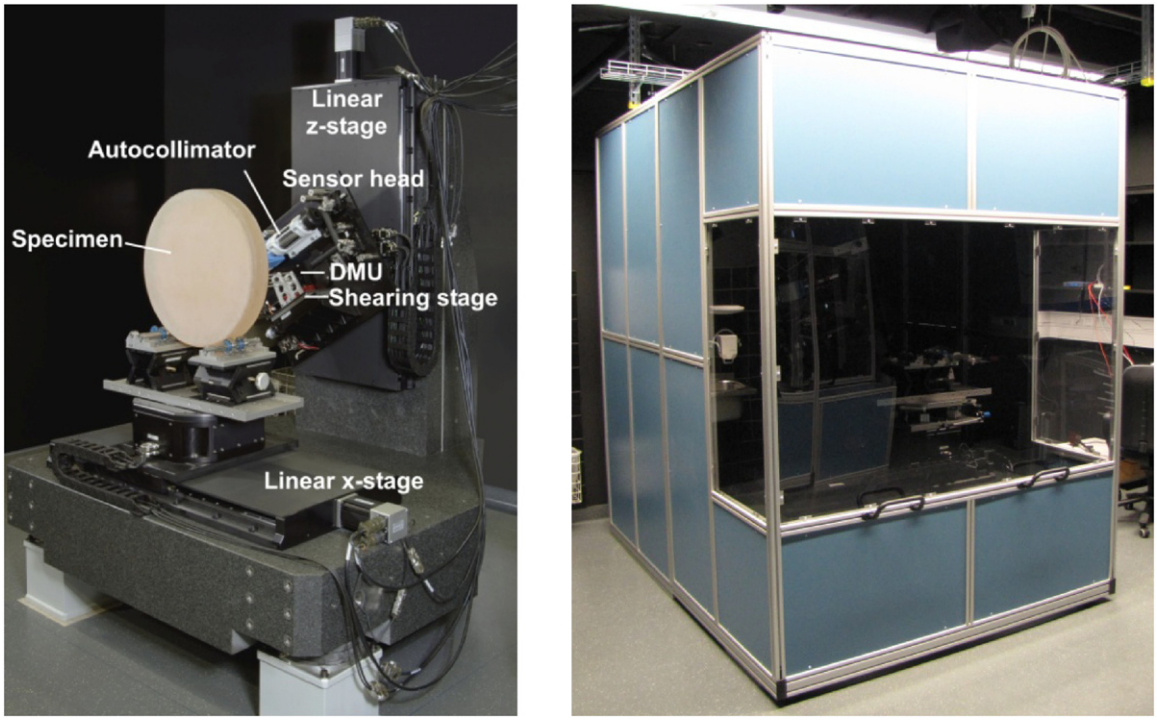

Figure 4. Photos of system 2 for vertical specimens (*left*: without housing; *right*: with housing).

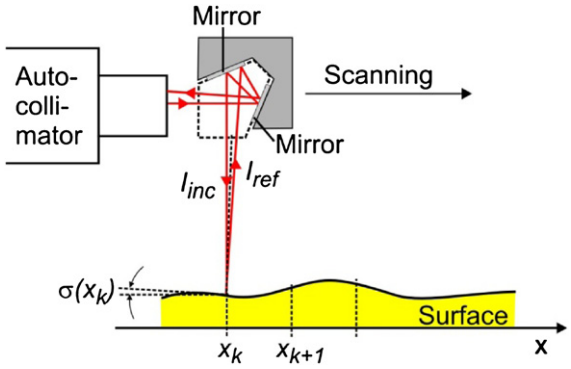

Figure 5. Direct deflectometric mode (pentaprism-based arrangement of the two deflection mirrors).

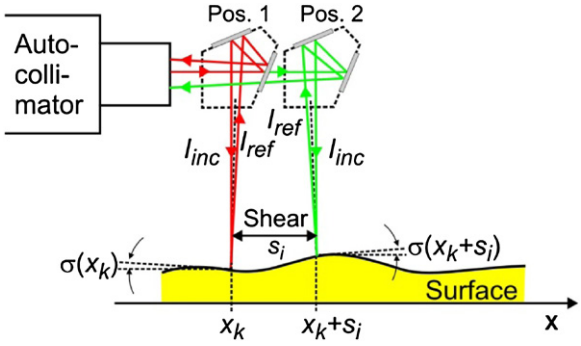

Figure 6. Difference deflectometric mode.

$\sigma(x_k)$ at each position x_k. Integration of the slopes $\sigma(x_k)$ yields the surface topography $h(x_k)$. The advantage of this method is the short measurement time. Disadvantages are that (*a*) the optical path length of the autocollimator beam changes during the measurement, which might cause additional angle measurement errors since the autocollimator is calibrated for a fixed distance and that (*b*) the measurement is affected by unavoidable specimen tilting during the measurement.

(2) In *difference deflectometric* mode (figure 6), slope differences between positions with fixed distances—the so-called shears—are measured. This procedure is also called the 'extended shear angle difference' (ESAD) method, because large lateral shears from mm to cm are used. The ESAD was invented at PTB more than 10 years ago and implemented in the ESAD measurement system [14–16]. In order to receive a unique solution, usually two shears $s_1 = \nu_1 \cdot \Delta x$ and $s_2 = \nu_2 \cdot \Delta x$ are required. The number of reconstructed points is $N = \nu_1 \cdot \nu_2$ [17]. Certain shear combinations are highly robust with respect to both random and systematic residual error influences on the difference data [9]. The measurement yields the following angle differences:

$$\Delta\sigma(x_k, s_i) = \sigma(x_k + s_i) - \sigma(x_k) \quad \text{with} \quad i = 1, 2$$

for $k = 1, 2, \ldots, n_i$.

From these differences, the slopes $\sigma(x_k)$ can be computed using the so-called natural extension to the full specimen length and shearing transfer functions [17]. Afterwards, the topography $h(x_k)$ can be calculated by the integration of these slopes $\sigma(x_k)$. Advantages of this method are that the measurement result is not influenced by possible specimen tilts during the scan—only during the difference measurement must the specimen be stable—and that the variation of the optical path length is limited to the applied shear length since the autocollimator 'follows' the DMU.

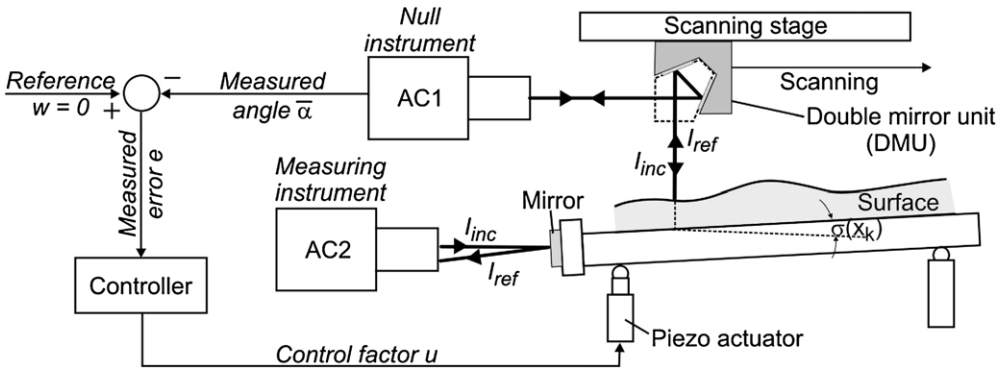

Figure 7. Exact autocollimation deflectometric scanning mode.

(3) With the new EADS mode (figure 7), the surface under test is kept perpendicular to the scanning beam by tilting the specimen with a piezoactuator [18]. The autocollimator AC1 is operated as a null instrument. The autocollimator AC2 measures the slopes $\sigma(x_k)$. Again, as in direct deflectometry, integration of the slopes $\sigma(x_k)$ yields the surface topography $h(x_k)$. A disadvantage of the EADS mode in comparison to the direct and the difference modes is its enlarged measuring time. Typical measuring times for each measuring point are 5 s for the direct deflectometric mode, 15 s for the difference mode and about 25 s for the EADS mode. The main advantages of this method compared to direct deflectometry are (*a*) that the optical path length of the angle measurement device (AC2) is constant, (*b*) that this angle can be measured with better accuracy since a greater measurement aperture can be used, and (c) that a smaller lateral resolution can be realized because the autocollimator AC1 (or another type of angle detector) acts as a null instrument only, and thus, only relative measurements around the zero value are needed.

4. Modelling

For the comparison of the different deflectometric modes and for the quantification of various error sources, we modelled the deflectometric flatness reference (DFR) system in a universal simulation environment, which is capable of simulating complete DFR measurements taking into account all significant mechanical and optical measurement and system parameters.

For the sensitivity analysis, we formed four groups of input quantities describing the properties of the scanning stage, the autocollimator, the double-mirror unit and the specimen. Table 1 shows the input quantities for the virtual experiments. This grouping of input quantities helps us to analyze the most significant influencing parameters.

In the simulations, it is assumed that the scanning stage has positional and angular errors (Δx, Δy, Δz, and $\Delta\alpha$, $\Delta\beta$, $\Delta\gamma$), which consist of systematic and stochastic parts. In a typical example, we assume a peak-to-valley value of 3 μm for the systematic positional errors, and a stochastic positional error of 0.3 μm (standard deviation of a normal distribution).

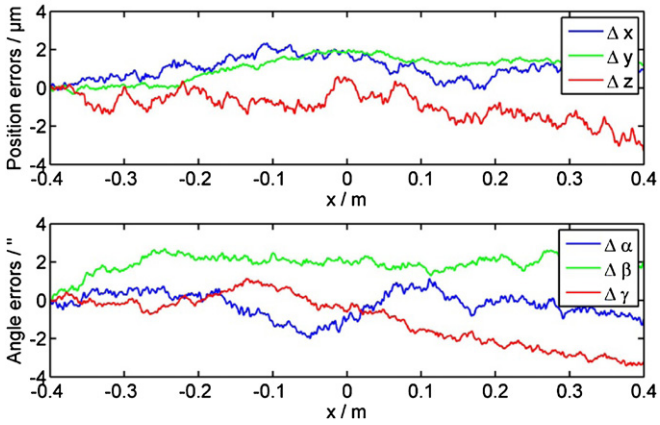

Figure 8. Example of systematic guidance (positional and angular) errors.

Typical systematic positional and angular errors are shown in figure 8.

The numerical values of the input quantities shown in table 1 are realistic estimates in order to assure a high validity and reliability of the virtual experiments. Figure 9 shows—in the form of so-called box plots—the results of a sensitivity analysis of direct deflectometry based on more than 100 virtual measurements of a specimen with a size of 800 mm. The box plots show the rms errors. The central mark is the median, and the edges of the box are the 25th and 75th percentiles. The ends of the whiskers represent the minimum and maximum data points. On the left-hand side of each of the four box plots, the respective error source is 'switched off' (ideal case) and on the right-hand side, the error is 'switched on' (real situation). The box plots reveal that the influence of each of the four parameter groups on the measured topography is of similar magnitude, and measurements at sub-nanometre level may be possible even for such large specimens.

5. Alignment of the mechanical and optical system

Non-perfect alignment of the measurement system results in systematic errors of the topography measurement. Simulations have shown that the alignment of the optical system must be in the arcsecond range in order to keep systematic topography errors in the sub-nanometre range [19]. Appropriate alignment

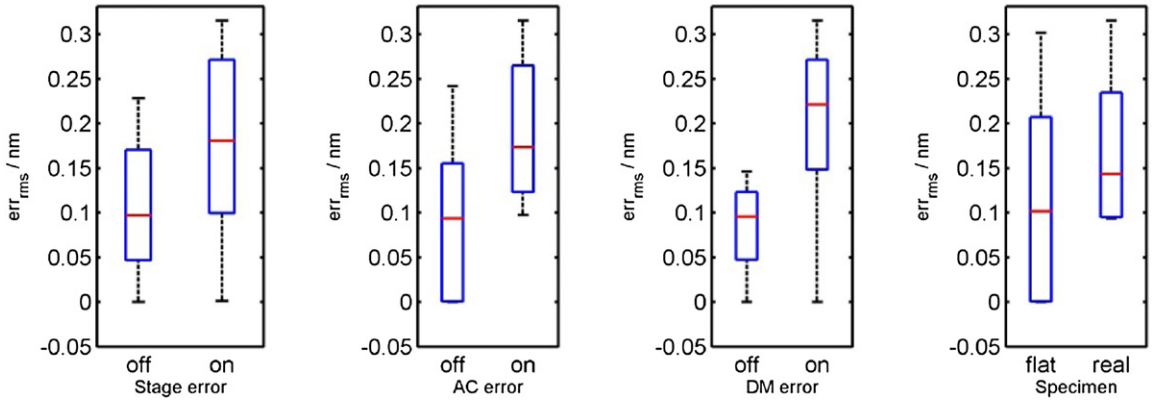

Figure 9. Typical sensitivity analysis of simulated topography measurements of an 800 mm specimen, for the four groups of input parameters (from left to right: guidance errors, autocollimator errors, errors of the double-mirror unit and influence of the specimen topography).

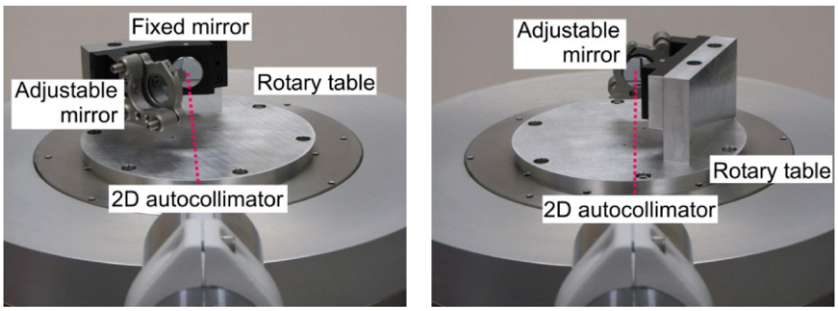

Figure 10. Alignment of the two mirrors of the DMU. *Left*: autocollimator faces the fixed mirror. *Right*: autocollimator faces the adjustable mirror.

Table 1. Input quantities for the virtual experiments.

Group	Input quantity	Values, errors	Distribution
1. Scanning stage	Position deviations	Length of axis: 1.75 m	
	$[\Delta x\ \Delta y\ \Delta z]$	Systematic: [3 3 3] μm	Random walk (pv)
		Stochastic: [0.3 0.3 0.3] μm	Normal distribution
	Angle deviations	Length of axis: 1.75 m	
	$[\Delta\alpha\ \Delta\beta\ \Delta\gamma]$	Systematic: [3 3 3] arcsec	Random walk (pv)
		Stochastic: [0.3 0.3 0.3] arcsec	Normal distribution
2. Autocollimator	Angle error of pitch	Stochastic: 0.003 arcsec	Normal distribution
	Angle error of yaw	Stochastic: 0.003 arcsec	Normal distribution
	Misalignment of AC and x-stage for all pitch, yaw and roll	Stochastic: 1 arcsec in pitch, yaw and roll	Normal distribution
3. Double mirror	Height of topography of mirror 1 and 2	Systematic: 10 nm (pv)	Random walk (pv)
	Spatial wavelengths of mirror 1 and 2	Systematic: [300 μm $\cdots$ 1 cm]	Random walk (pv)
4. Specimen*	Height of topography for a 1 m specimen	Systematic: 400 nm (pv)	Random walk (pv)
	Spatial wavelengths	Systematic: [300 μm $\cdots$ 1 m]	Random walk (pv)

*The specimen is aligned perfectly with the optical beam.

strategies of deflectometric systems have already been published [20–22], which need, however, to be refined for the new DRF systems. The alignment procedure consists of three steps: (a) alignment of the DMU itself, (b) alignment of the mechanical scanning stage with respect to the optical axis and (c) alignment of the DMU with respect to the optical axis.

For the alignment of the two mirrors of the DMU, the device is mounted on a highly accurate rotary table (LT Ultra RT 300 with an encoder Heidenhain RON 886, accuracy better than 0.2 arcsec), see figure 10. The stage is rotated so that the autocollimator beam faces a part of the fixed mirror of the DMU. The autocollimator is adjusted to obtain a zero reading for the x- and y-axes. Then, the double mirror is rotated with the rotary stage by 135°. Consequently, the autocollimator beam now faces the adjustable mirror of the DMU, which is then adjusted so that the autocollimator again indicates zero. With this procedure, it is possible to align the two mirrors with arcsec accuracy. The two mirrors were made up of polished silicon substrates from Gooch and Housego (www.goochandhousego.com) coated by an aluminium and

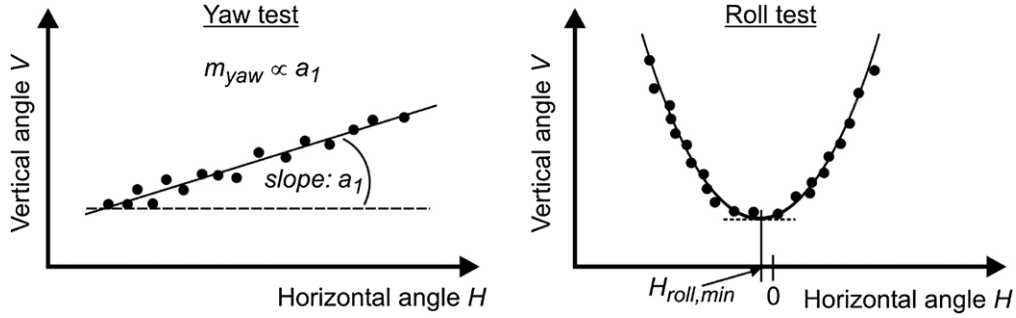

Figure 11. Principle of the yaw and roll test.

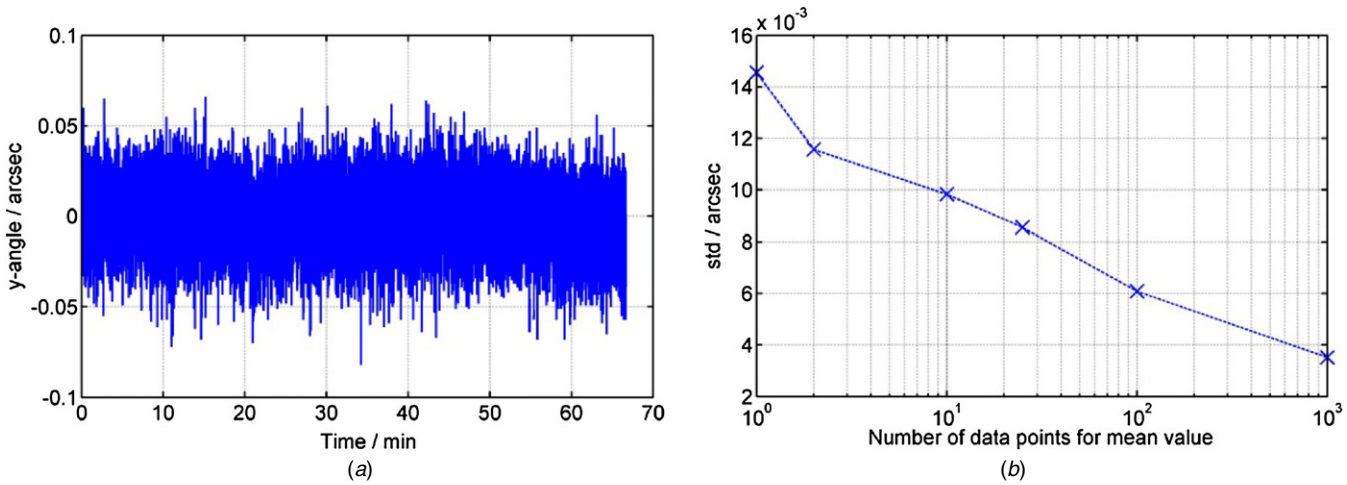

Figure 12. Measurement of the point stability of system 1.

a SiO_2 protection layer. The flatness of the inner part of the mirrors is better than $\lambda/100$.

The alignment of the autocollimator beam with respect to the scanning axis (beam and scanning axis must be parallel to each other) is accomplished by using an image sensor, which is mounted at carriage 2 (see figure 3). The alignment criterion is that the centre of gravity of the beam spot position on the image sensor remains constant when moving the image sensor along the scanning axis.

To align the DMU with respect to the autocollimator beam, the so-called yaw and roll tests are used (see figure 11). When the yaw angle of the DMU is varied, the horizontal and vertical angle readings of the autocollimator show linear behaviour as a function of the yaw angle. The slope m_{yaw} of this yaw test is given by the difference of the roll angle of the specimen a_{sp} and the roll angle of the autocollimator a_{ac}. The aim of this test is to ensure that the slope of this linear relationship is zero, and thus, the roll angle of the specimen and autocollimator are well aligned. Rotating the DMU around the roll angle leads to quadratic behaviour of the autocollimator readings. If the slope m_{yaw} of the yaw test is zero, then the value $H_{\mathrm{roll,min}}$ is given by the difference of the yaw angle of the double-mirror unit γ_{dmu} and the autocollimator γ_{ac}. Hence, if $H_{\mathrm{roll,min}} = 0$ is obtained, then the yaw angles of the double-mirror unit and the autocollimator are well aligned. These alignment procedures are described in detail in previous publications [17, 18].

6. Measurements

The first test measurements were performed using the DFR system 1. The measurements are fully automated so that no person must be inside the laboratory during the measurements. This allows temperature stabilities of 0.1 to 0.2 K over 24 h. Figure 12(*a*) shows the results of point stability tests, where autocollimator readings have been recorded over a period of 1 h without scanning the DMU. As expected for noise-dominated errors, the standard deviation of the measured mean angle decreases with increasing number of data points used for averaging (figure 12(*b*)). Averaging over 100 successive angle values (meaning 4 s measurement time based on the autocollimator's sampling rate of 25 Hz) results in a standard deviation of 6 ms.

With the direct deflectometric method, we measured the topography of a specimen with a diameter of about 540 mm (see the specimen in figure 3). In total, seven repeated measurement scans along one direction were performed. The step size was 1 mm, and at each position, the measured slope angles were averaged over 4 s; each scan took about 40 min. The seven measured slope scans and their differences to the averaged slope scan are shown in figure 13: the differences are in the range of 0.01 arcsec. The resulting topography, shown in figure 14(*a*), has standard deviations ranging from 0.3 to 0.65 nm (figure 14(*b*)), thus demonstrating sub-nanometre repeatability with these first test measurements.

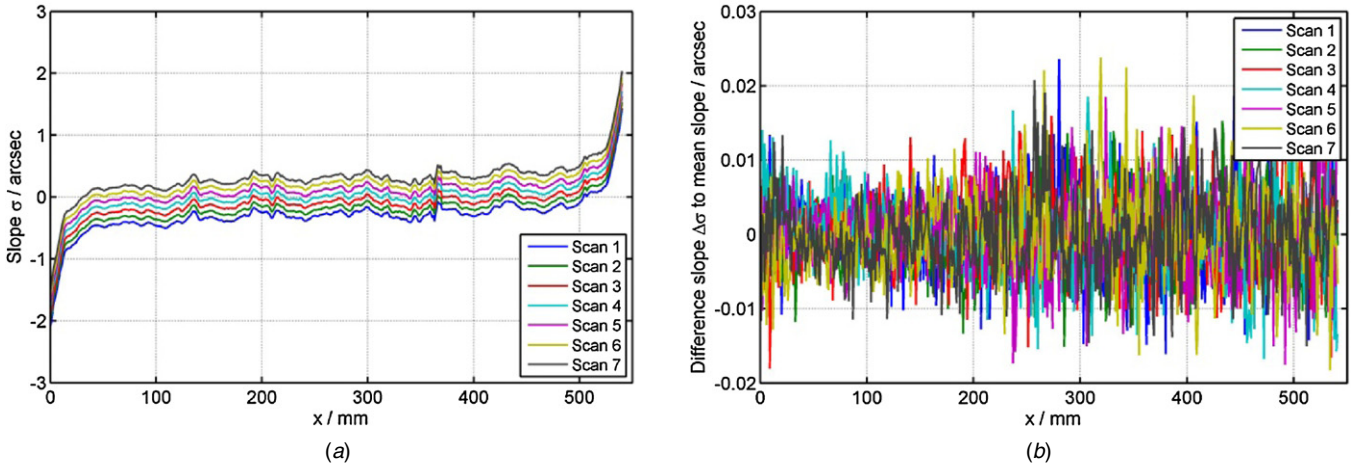

Figure 13. Repeated measurements of a specimen with a size of about 540 mm: (*a*) measured slopes are shown with an additional shift equal to 0.1 arcsec between each scan for better visualisation and (*b*) differences between the scans.

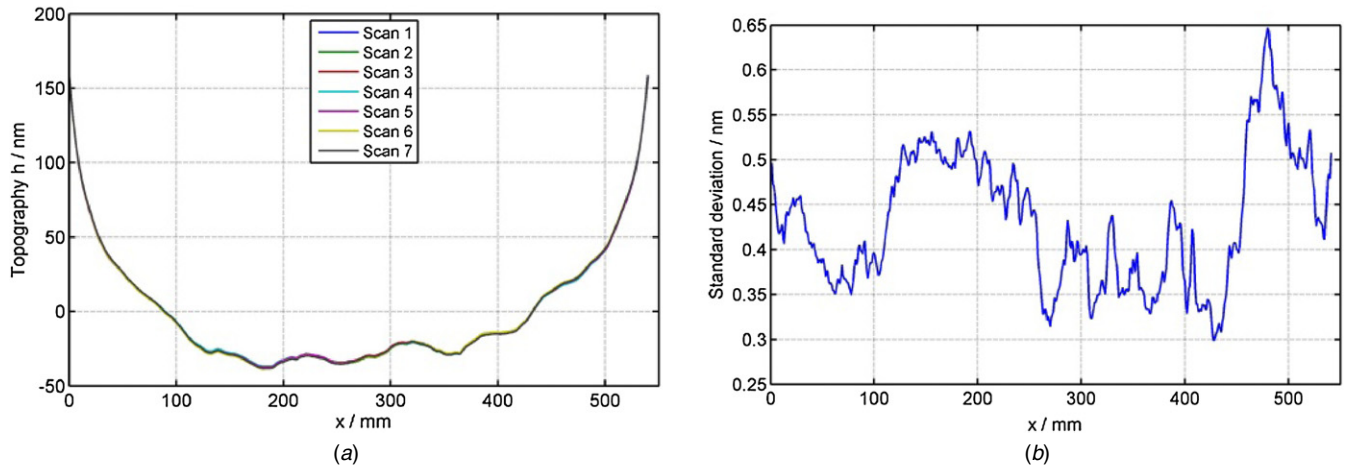

Figure 14. (*a*) Resulting topography obtained by integration of the measured slopes. (*b*) Standard deviation of the 7 scans.

7. Conclusion and outlook

Two new scanning deflectometric measurement systems have been installed at PTB. The systems were designed and built up based on simulation data to define and specify the mechanical and optical components. Special and optimized alignment procedures have been developed to adjust the systems with arcsecond accuracy. The first test measurements show sub-nanometre repeatability when measuring large (>500 mm) specimens. Possible further improvements are currently being investigated by installing a new holder for the DMU and by shielding the optical path. In addition, a complete measurement uncertainty budget shall be established. Some input quantities are listed in table 1. Further input quantities, such as climatic conditions or integration errors, will be estimated. As part of the European Metrology Research Programme (EMRP), the project 'optical and tactile metrology for absolute form characterisation' [23] aims to decrease the lateral resolution of the EADS method to about 0.1 mm [24]. This requires new low-noise angular null sensors to be designed and developed within this EMRP project, which is jointly funded by the EMRP participating countries within EURAMET and the European Union.

References

[1] Erko A, Idir M, Krist T and Michette A G 2008 chapter 10: The long trace profilers, chapter 11: The nanometer optical component measuring machine *Modern Developments in X-Ray and Neutron Optics (Springer Series in Optical Sciences* vol 137*)* (Berlin: Springer) pp 181–200

[2] Alcock S G, Sawhney K J S, Scott S, Pedersen U, Walton R, Siewert F, Zeschke T, Senf F, Noll T and Lammert H 2009 The diamond-NOM: a non-contact profiler capable of characterizing optical figure error with sub-nanometre repeatability *Nucl. Instrum. Methods Phys. Res.* A **616** 224–8

[3] Schulz G and Schwider J 1967 Precise measurement of planeness *Appl. Opt.* 6 1077–84

[4] Schulz G, Schwider J, Hiller C and Kicker B 1971 Establishing an optical flatness standard *Appl. Opt.* **10** 929–34

[5] Griesmann U 2006 Three-flat test solutions based on simple mirror symmetry *Appl. Opt.* **45** 5856–65

[6] Griesmann U 2007 Three-flat tests including mounting-induced deformations *Opt. Eng.* **46** 093601

[7] Vannoni M and Molesini G 2007 Iterative algorithm for three flat test *Opt. Express* **15** 6809–16

[8] Vannoni M and Molesini G 2008 Three-flat test with plates in horizontal posture *Appl. Opt.* **47** 2133–45

[9] Geckeler R D and Weingärtner I 2002 Sub-nm topography measurement by deflectometry: flatness standard and wafer nanotopography *Proc. SPIE* **4779** 1–12
[10] Probst R, Wittekopf R, Krause M, Dangschat H and Ernst A 1998 The new PTB angle comparator *Meas. Sci. Technol.* **9** 1059–66
[11] Just A, Krause M, Probst R and Wittenkopf R 2003 Calibration of high-resolution electronic autocollimators against an angle comparator *Metrologia* **40** 288–94
[12] Ehret G, Schulz M, Baier M and Fitzenreiter A 2009 A new optical flatness reference measurement system *Proc. 110 Jahrestagung der Deutschen Gesellschaft für Angewandte Optik (DGaO)* http://www.dgao-proceedings.de/download/110/110_p22.pdf
[13] Schulz M, Ehret G, Stavridis M and Elster C 2010 Concept, design and capability analysis of the new deflectometric flatness reference at PTB *Nucl. Instrum. Methods Phys. Res.* A **616** 134–9
[14] Weingärtner I, Schulz M and Elster C 1999 Novel scanning technique for ultra-precise measurement of topography *Proc. SPIE* **3782** 306–17
[15] Weingärtner I, Loheide S and Schulz M 2000 Verfahren zur bestimmung der topographie einer wenigstens nahezu planaren oberfläche *Patent* DE19833269C1
[16] Geckeler R, Weingärtner I, Just A and Probst R 2001 Use and traceable calibration of autocollimators for ultra-precise measurement of slope and topography *Proc. SPIE* **4401** 184–95
[17] Elster C and Weingärtner I 1999 Solution to the shearing problem *Appl. Opt.* **38** 5024–31
[18] Schulz M, Ehret G and Fitzenreiter A 2010 Scanning deflectometric form measurement avoiding path-dependent angle measurement errors *J. Eur. Opt. Soc.: Rapid Publ.* **5** 10026
[19] Ehret G, Schulz M, Stavridis M and Elster C 2009 A new flatness reference measurement system based on deflectometry and difference deflectometry *Fringe: 6th Int. Workshop on Advanced Optical Metrology* pp 318–23
[20] Geckeler R D 2007 Optimal use of pentaprisms in highly accurate deflectometric scanning *Meas. Sci. Technol.* **18** 115–25
[21] Ehret G, Schulz M, Fitzenreiter A, Baier M, Jöckel W, Stavridis M and Elster C 2011 Alignment methods for ultraprecise deflectometric flatness metrology *Proc. SPIE* **8082** 808213
[22] Barber S K, Geckeler R D, Yashchuk V V, Gubarev M V, Buchheim J, Siewert F and Zeschke T 2011 Optimal alignment of mirror-based pentaprisms for scanning deflectometric devices *Opt. Eng.* **50** 073602
[23] EMRP-Project 09/2011–08/2014 Optical and tactile metrology for absolute form characterization http://www.ptb.de/emrp/ind10-home.html
[24] Schulz M, Ehret G, Baier M and Fitzenreiter A 2011 Deflectometric measurement of flat and slightly curved optical surfaces with improved lateral resolution *VDI-Ber.* **2156** 113–8